Journal of Alloys and Compounds 522 (2012) 30–34

Contents lists available at SciVerse ScienceDirect

Journal of Alloys and Compounds

journal homepage: www.elsevier.com/locate/jallcom

Green upconversion luminescence from poly-crystalline Yb^{3+}, Er^{3+} Co-doped $CaMoO_4$

Jun Ho Chung[a], Jeong Ho Ryu[b], Jong Won Eun[a], Jeong Hoon Lee[a], Sang Yeop Lee[a], Tae Hyung Heo[a], Bong Geun Choi[a], Kwang Bo Shim[a,*]

[a] Department of Materials Science and Engineering, Hanyang University, 17 Haengdang-dong, Seongdong-gu, Seoul 133-791, South Korea
[b] Department of Materials Science and Engineering, Korea National University of Transportation, 50 Daehak-ro, Chungji-si, Chungbuk 380-702, South Korea

ARTICLE INFO

Article history:
Received 13 December 2011
Received in revised form 10 January 2012
Accepted 10 January 2012
Available online 28 January 2012

Keywords:
Green upconversion (UC) luminescence
Er^{3+}/Yb^{3+} co-doped $CaMoO_4$
UC luminescent mechanism

ABSTRACT

The upconversion (UC) luminescence properties of polycrystalline Er^{3+}/Yb^{3+} co-doped $CaMoO_4$ synthesized by a complex citrate gel method were investigated in detail. Under 980 nm excitation, Er^{3+}/Yb^{3+} co-doped $CaMoO_4$ has exhibited a weak red emission near 670 nm and strong green UC emissions at 530 and 550 nm, corresponding to the intra 4f transitions of Er^{3+} ($^4F_{9/2}$, $^2H_{11/2}$, $^4S_{3/2}$) → Er^{3+} ($^4I_{15/2}$). The optimum doping concentrations of Er^{3+} and Yb^{3+} were determined to result in the highest UC luminescence and a possible UC mechanism of Er^{3+}/Yb^{3+} co-doped $CaMoO_4$ depending on the pump power dependence is discussed in detail.

1. Introduction

Over the past several decades, rare earth (RE)-doped upconversion (UC) luminescence has received considerable attention because of their potential applications including three-dimensional displays [1], laser and optical amplifiers [2], solar cells [3,4], and bio-technologies [5,6]. Many RE ions have been researched as luminescent centers for UC materials. Among them, Er^{3+}-doped UC phosphors are very popular due to their abundant energy level for UC luminescence and high luminescent quenching concentration compared to other RE ions [7]. However, because Er^{3+} ions have a very low absorption cross-section of the $^4I_{11/2}$ level under 980 nm excitation, Er^{3+} single-doped UC phosphors have a relatively low emission intensity and pump efficiency. In order to overcome these drawbacks and enhance the UC emission efficiency, Yb^{3+} ions are generally used as co-dopant ions because they have a large absorption cross-section around 980 nm and a possible effective energy transfer from Yb^{3+} to the activator ions through the multi photon process [8,9].

The selection of the host matrix is another important factor to obtain highly efficient UC luminescence because the different crystal fields caused by structural symmetry of the host materials can contribute to inner shell transitions such as intra 4f–4f transitions in RE ions. Up to now, most of the RE-doped UC phosphors have been studied with halides [10], glasses [11] and chalcogenides [12]. However, their production costs are high and they have poor chemical stabilities [13], restricting their use in practical application. Recently, metal oxides have been investigated as the host matrices of UC materials because they have very low excitation thresholds and are very chemically, mechanically, and thermally stable.

Scheelite structural materials are important inorganic materials which have high application potential in various fields including photoluminescence and electro-optic applications [14,15]. Bivalent cations relatively larger than Mo^{6+} cations exist in the so-called scheelite structure, where the Mo^{6+} ions are in tetrahedral coordination with oxygen ligands, while bivalent metal atoms have polyhedral coordination. Among them, $CaMoO_4$ has a high density (4.25 g/cm^3), high irradiation, thermo-luminescence, and relatively low phonon threshold energy compared to other oxide materials [16,17]. The Mo^{6+} ions in $CaMoO_4$ matrices have a strong polarization induced by the large electric charge and small radius, which consequently decrease the symmetry and enhance the stark energy splitting in the crystal field [18]. Therefore, we expected that $CaMoO_4$ can be a good match for UC matrices. However, the UC luminescence of Er^{3+}/Yb^{3+} co-doped polycrystalline $CaMoO_4$ has not been studied yet. Consequently, realization of efficient near infrared (NIR) to visible UC luminescence in $CaMoO_4$ will have great impact on the utilization of its potential advantages.

In this work, we investigated UC luminescence while varying the Er^{3+} and Yb^{3+} ion concentrations in $CaMoO_4$ matrices that were synthesized by a complex citrate gel method with microwave

* Corresponding author. Tel.: +82 2 2220 0501; fax: +82 2 2291 7395.
E-mail address: kbshim@hanyang.ac.kr (K.B. Shim).

0925-8388/$ – see front matter © 2012 Elsevier B.V. All rights reserved.
doi:10.1016/j.jallcom.2012.01.059

assistance. The properties of the structure and photoluminescence under 980 nm excitation are discussed. Moreover, the effects of the Er^{3+} and Yb^{3+} concentrations on UC emission intensity and the related possible UC mechanism are presented in detail.

2. Experimental procedure

2.1. Starting materials

Er^{3+}/Yb^{3+} co-doped $CaMoO_4$ powders were synthesized by a complex citrate gel method with microwave assistance. Calcium nitrate ($Ca(NO_3)_2{\cdot}4H_2O$, 99.99%, Junsei Chemical Co. Ltd., Japan), ammonium para-molybdate ($(NH_4)_6{\cdot}Mo_7O_{24}{\cdot}4H_2O$, 99.99%, Wako Chemical Co. Ltd., Japan), ytterbium chloride hydrate ($YbCl_3{\cdot}xH_2O$ ($x=6$), 99.99%, Alfa Aesar), and erbium nitrate pentahydrate ($Er(NO_3){\cdot}5H_2O$, 99.99%, Alfa Aesar) were used as the metallic cations. DI water and citric acid ($HOC(CO_2H)(CH_2CO_2H)_2$, CA, 99.9%, Yukiri Pure Chemical Co. Ltd., Japan) were used as the solvent and chelating agent, respectively.

2.2. Preparation and synthesis of Er^{3+}/Yb^{3+} co-doped $CaMoO_4$

First, for the investigation of the UC luminescence with various Er^{3+} concentrations, the doping level of Yb^{3+} ions in the $CaMoO_4$ matrices was fixed at 8 mol%. The molar ratios of the cations were varied as follows.

$$Ca_{1-x}(Er_x + Yb_{0.08})MoO_4\ (x = 0,\ 0.01,\ 0.02,\ 0.03,\ 0.05) \quad (1)$$

Then, to confirm the effect of Yb^{3+} concentration on UC luminescence in $CaMoO_4$, the concentration of Er^{3+} ions in the $CaMoO_4$ matrices was fixed at 2 mol% while the following cation concentrations were investigated.

$$Ca_{1-y}(Er_{0.02} + Yb_y)MoO_4\ (y = 0,\ 0.04,\ 0.08,\ 0.12,\ 0.16,\ 0.20,\ 0.25) \quad (2)$$

For the experiments, a solution was kept at 100 °C for 10 min under constant stirring until it became viscous. The solution was treated microwave for 10 cycles with on-time duration of 2 min and off-time duration of 1 min in ambient atmosphere until the solution became to gel. After microwave treatment, obtained gel was heated in oven at 250 °C during 24 h for removing organic substance and evaporating moisture until the yellow dried powders were gained (hereafter referred to as 'precursors') were obtained. The precursors were calcined at various temperatures ranging from 300 to 700 °C for 3 h in the ambient atmosphere.

2.3. Characterization

The phase analysis was conducted using X-ray diffraction (XRD, Rigaku D/MAX2C, Japan, Cu-α ($\lambda = 1.5046$ Å)). The morphology and microstructure were observed by a scanning electron microscopy (SEM, JEOL JSM-5900LV, Japan). Room-temperature UC luminescent spectra were obtained using a photoluminescence spectrophotometer (PerkinElmer, LS55 with a 100 mW laser diode, USA) in the range of 400–700 nm under 980 nm laser excitation. The pump power dependence was calculated as the irradiation power from 20 to 110 mW (SPEX, 1404p, France).

3. Results and discussion

3.1. Structural and morphological analysis of Er^{3+}/Yb^{3+} co-doped $CaMoO_4$

Fig. 1 shows the phase identification of $CaMoO_4$ heat-treated for 3 h with respect to the heating temperature, as determined by XRD. The $CaMoO_4$ powders heat-treated at 300 °C were amorphous with no crystallized phases. However, above a temperature of 400 °C, the characteristic $CaMoO_4$ phase appeared, and all of the prominent peaks corresponding to the $CaMoO_4$ phases were clearly observed above 600 °C, without any peaks assigned to either CaO or MoO_3 phase, which is in good agreement with the standard patterns of $CaMoO_4$ in JCPDS No. 77-2243. The XRD results demonstrate that the crystallization of the $CaMoO_4$ precursors was completed at a temperature of 600 °C, which is much lower than that of samples prepared by a conventional solid-state reaction (about 900–1000 °C) [19].

For investigation of particle size and morphology, SEM images of Er^{3+}/Yb^{3+} co-doped $CaMoO_4$ calcined at 600 °C for 3 h are shown in Fig. 2. Fig. 2 shows that the average particle size of specimen has analogous size about several hundred nanometers and uniform spherical shapes.

Fig. 3 shows the phase analysis of $CaMoO_4$ with (a) various Er^{3+} concentrations up to 5 mol% fixed at 8 mol% Yb^{3+} and (b) various

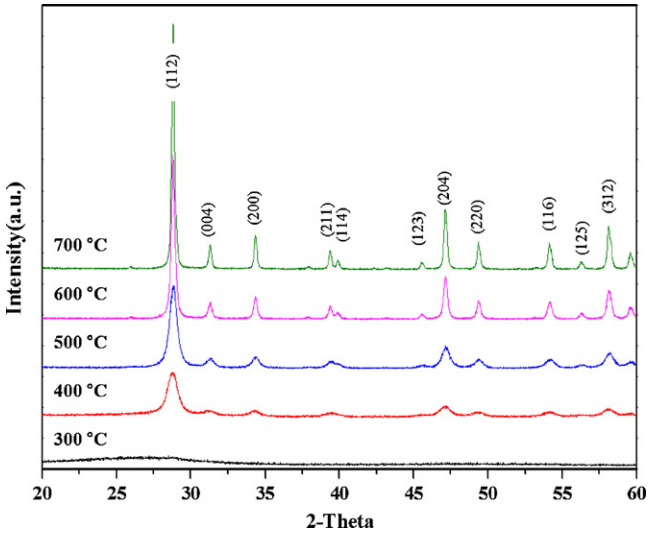

Fig. 1. X-ray diffraction patterns of $CaMoO_4$ UC phosphors calcined at temperatures ranging from 300 to 700 °C for 3 h.

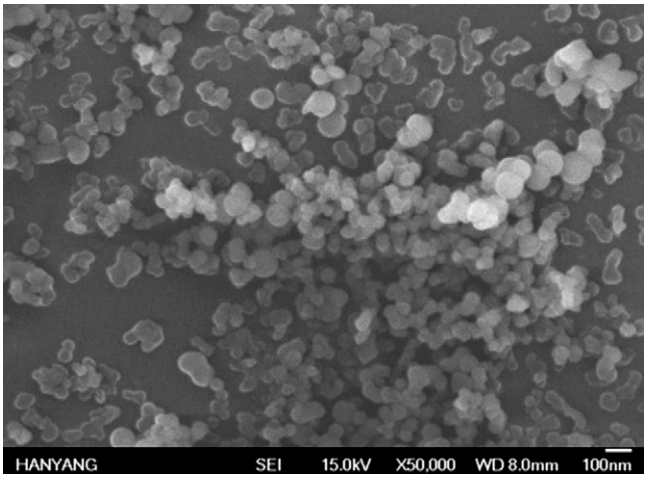

Fig. 2. SEM images of Er^{3+}/Yb^{3+} (2/16 mol%) co-doped poly-crystalline $CaMoO_4$ UC phosphors.

Yb^{3+} concentrations up to 20 mol% fixed at 2 mol% Er^{3+} calcined at 600 °C for 3 h, as determined by XRD. No impurities or secondary phases could be identified, which is evidence that single phase $CaMoO_4$:Er^{3+}/Yb^{3+} with Er^{3+} and Yb^{3+} concentrations up to 5 and 20 mol% can be obtained. These powders fundamentally maintain characteristic of scheelite structure, which are not affected by the doped lanthanide ions [20]. However, as shown in the inset in Fig. 3, with higher Er^{3+}/Yb^{3+} concentrations, the diffraction peaks are shifted to a high 2θ angle, which illustrates that Er^{3+}/Yb^{3+} ions were well substituted into Ca^{2+} ion sites, resulting in reduced lattice constants. Moreover, broadening of the diffraction peaks at (1 1 2) with increasing Er^{3+}/Yb^{3+} concentration shows that higher doping concentrations of the Er^{3+}/Yb^{3+} ions lead to decreased crystallinity.

3.2. Upconversion luminescence properties of Er^{3+}/Yb^{3+} co-doped $CaMoO_4$

Fig. 4 shows room temperature UC luminescent spectra of the Er^{3+}/Yb^{3+} co-doped $CaMoO_4$ (a) with Er^{3+} concentrations ranging from 0 to 5 mol% fixed with 8 mol% Yb^{3+} and (b) Yb^{3+} concentrations ranging from 0 to 25 mol% fixed with 2 mol% Er^{3+} under excitation at 980 nm. The UC luminescent spectra of the Er^{3+}/Yb^{3+}

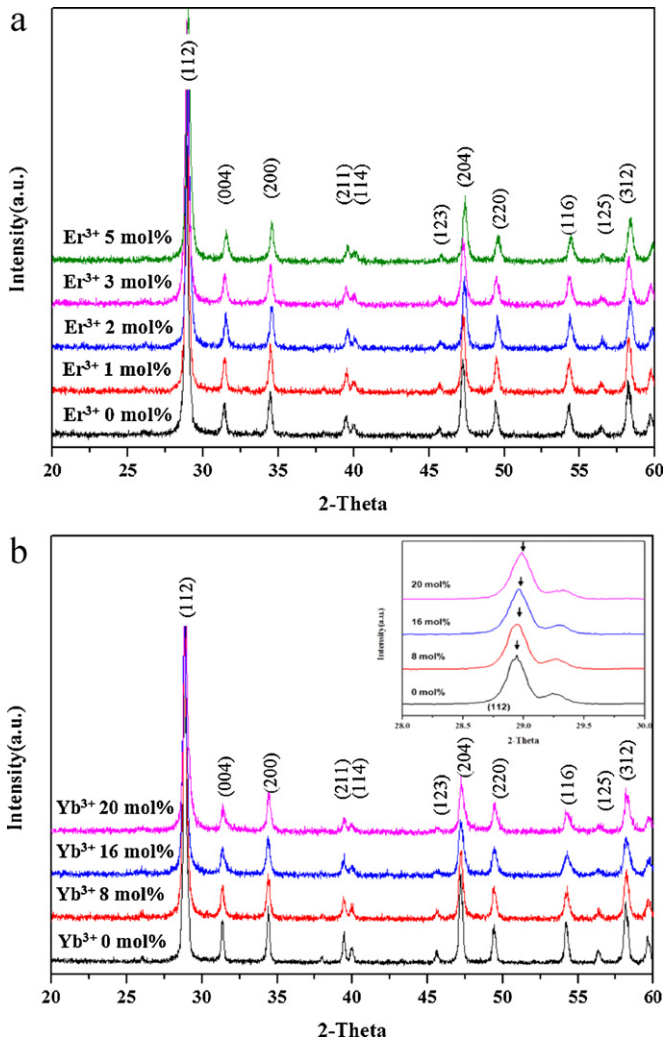

Fig. 3. X-ray diffraction patterns of $CaMoO_4$ UC phosphors with (a) Er^{3+} concentrations of 0–5 mol% and (b) Yb^{3+} concentrations of 0–20 mol%. The inset of Fig. 2(b) represented that main diffraction peaks of (1 1 2) plane near $2\theta = 29^{\circ}$ with increasing Yb^{3+} concentrations.

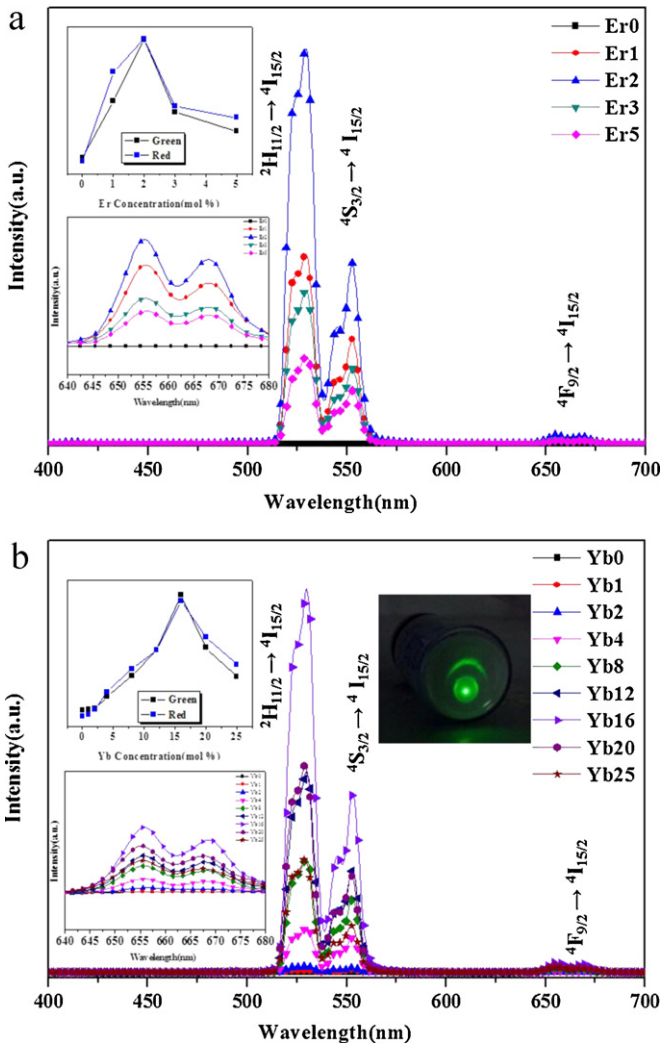

Fig. 4. Photoluminescence spectra (PL) of $CaMoO_4$ UC phosphors with (a) various Er^{3+} concentrations with a fixed Yb^{3+} concentration of 8 mol% and (b) various Yb^{3+} concentrations with a fixed Er^{3+} concentration of 2 mol%. The photographs in the inset show the Er^{3+}/Yb^{3+} (2/16 mol%) co-doped $CaMoO_4$ sample and photoluminescence of red emission ranging from 640 to 680 nm with various dopants concentrations.

co-doped $CaMoO_4$ consisted of three regions [21]: (1) green emissions near 530 nm assigned to the $^2H_{11/2} \rightarrow {}^4I_{15/2}$ transition, (2) an intense green emission near 550 nm attributed to the $^4S_{3/2} \rightarrow {}^4I_{15/2}$ transition, and (3) relatively weak red emission around 656 and 670 nm attributed to the $^4F_{9/2} \rightarrow {}^4I_{15/2}$ transition, which contribute to the intra 4f–4f transitions of Er^{3+} ions. All emission bands are accompanied by several well resolved Stark levels in Er^{3+}. As seen in Fig. 4, the UC emission intensity of green emissions near 530 and 550 nm and red emissions around 656 and 670 nm increased with increasing Er^{+3+}/Yb^{3+} concentration from 0/0 to 2/16 mol% and then decreased beyond 2/16 mol% due to the concentration quenching effect [22]. The concentration quenching effect can be explained by the energy transfer between nearest Er^{3+} and Yb^{3+} ions. That is, with increasing Er^{3+} and Yb^{3+} ion concentrations, the distance between Er^{3+} and Yb^{3+} ions will decrease, which can promote non-radiative energy transfer such as an exchange interaction or multipole–multipole interactions [22]. Such a result is also observed from Er^{3+} doped and Er^{3+}/Yb^{3+} co-doped in other host matrices [23,24]. The concentration dependence of upconversion emissions could be mainly attributed to the interactions between doping ions. Therefore, according to above mentioned results, the optimum Er^{3+}/Yb^{3+} doping concentration was found to be 2/16 mol%. The Er^{3+}/Yb^{3+} co-doped $CaMoO_4$ (2/16 mol%) specimen exhibited a strong green emission visible to the naked eye when excited by a 980 nm laser diode (100 mW), as shown in inset of Fig. 4(a).

Fig. 5 shows the green and red UC luminescent intensities of $CaMoO_4$ co-doped with a Er^{3+}/Yb^{3+} concentration up to 2/16 mol% plotted on the logarithmic scale as a function of pump power. The UC process, I, is proportional to the exponent of P, n, as shown below [23].

$$I \propto P^n \tag{3}$$

In this equation, n is the number of pumping photons required to excite the emitting state, I is the luminescent intensity, and P is the laser pumping power. The calculated n values are 1.68, 1.70, 1.55, and 1.59 for green emissions at 530 and 550 nm and red emissions at 656 and 670 nm, respectively. The n values for green emission at 530 nm ($^4I_{11/2} \rightarrow {}^4I_{15/2}$) and 550 nm ($^4S_{3/2} \rightarrow {}^4I_{15/2}$) are close to 2, while the n values for red emission at 656 nm and 670 nm ($^4F_{9/2} \rightarrow {}^4I_{15/2}$) are slightly smaller than that of green emissions, which are in good agreement with previous n values obtained for

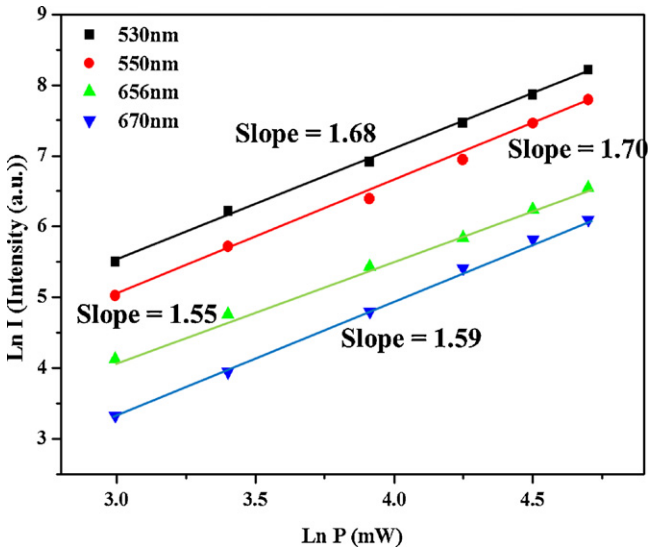

Fig. 5. Power dependence of the upconversion emission intensities of Er^{3+}/Yb^{3+} (2/16 mol%) co-doped $CaMoO_4$ at 530, 550, 656, and 670 nm.

green and red emissions in Er^{3+} ions [24]. These results indicate that the UC mechanism corresponding to green and red emissions occurs via a two photon process.

3.3. Possible upconversion mechanism of Er^{3+}/Yb^{3+} co-doped $CaMoO_4$

To better comprehend the mechanism which populates the green ($^2H_{11/2}$, $^4S_{3/2} \rightarrow {}^4I_{15/2}$) and red ($^4F_{9/2} \rightarrow {}^4I_{15/2}$) UC luminescence, the UC emission mechanism and population processes of the Er^{3+}/Yb^{3+} co-doped $CaMoO_4$ system are schematically illustrated in Fig. 6. Under 980 nm excitation, Er^{3+} and Yb^{3+} ions are initially excited from the ground state to the excited state through the ground state absorption (GSA) process (Er^{3+}: $^4I_{15/2} \rightarrow {}^4I_{11/2}$,$Yb^{3+}$: $^2F_{7/2} \rightarrow {}^2F_{5/2}$) or the energy transfer (ET) process of $^2F_{5/2}(Yb^{3+}) + {}^4I_{15/2}(Er^{3+}) \rightarrow {}^2F_{7/2}(Yb^{3+}) + {}^4I_{11/2}(Er^{3+})$ are responsible for the population at the $^4I_{11/2}$ level in Er^{3+}. For the green emissions, there are three possible processes for the energy transition from the $^4I_{11/2}$ level to the $^4F_{7/2}$ level of Er^{3+}, as follows [25–27].

$$\text{ESA}: {}^4I_{11/2} + \text{a photon (980 nm)} \rightarrow {}^4F_{7/2} \quad (4)$$

$$\text{ET}: {}^2F_{5/2}(Yb^{3+}) + {}^4I_{11/2}(Er^{3+}) \rightarrow {}^2F_{7/2}(Yb^{3+}) + {}^4F_{7/2}(Er^{3+}) \quad (5)$$

$$\text{ET}: {}^4I_{11/2}(Er^{3+}) + {}^4I_{11/2}(Er^{3+}) \rightarrow {}^4F_{7/2}(Er^{3+}) + {}^4I_{15/2}(Er^{3+}) \quad (6)$$

These three possible processes populate from the $^4I_{11/2}$ level to the $^4F_{7/2}$ level in the Er^{3+} level, and then the $^4F_{7/2}$ level relaxes rapidly and non-radiatively to the next lower levels at $^2H_{11/2}$ and $^4S_{3/2}$ in Er^{3+} because of short lifetime of the $^4F_{7/2}$ level [28]. As a result, the above processes can produce green emissions in the spectral lines near 530 and 550 nm through the radiative transitions of $^2H_{11/2}/{}^4S_{3/2} \rightarrow {}^4I_{15/2}$. For the red emission, the $^4F_{9/2}$ level is generated by non-radiative relaxation from the $^4S_{3/2}$ to the $^4F_{9/2}$ level and cross relaxation (CR) via the $^4F_{7/2} + {}^4I_{11/2} \rightarrow {}^4F_{9/2} + {}^4F_{9/2}$ transition in Er^{3+}[29]. Finally, the $^4F_{9/2}$ level relaxes radiatively to the ground state at the $^4I_{15/2}$ level and releases red emission at 656 and 670 nm, as shown in Fig. 4(a and b). The UC emission is dominated to strong green emission at 530 ($^2H_{11/2} \rightarrow {}^4I_{15/2}$) and 550 nm ($^4S_{3/2} \rightarrow {}^4I_{15/2}$). The red emissions are very weak due to the weak absorption cross-section of the $^4I_{13/2}$ level [30]. Moreover, as the Er^{3+} and Yb^{3+} concentration increases up to 2/16 mol%, the green UC emission dramatically increases compared to the red emission. This is possibly due to the probability of electrons in the $^4I_{11/2}$ level being populated to the $^4F_{7/2}$ level via the energy transfer upconversion (ETU) process, which is much higher than that of non-radiative relaxation to the $^4I_{13/2}$ level [30]. It is worth noting that $CaMoO_4$ can be great candidate for green UC phosphors and played an important role in the industrial fields that need green UC phosphors because Er^{3+}/Yb^{3+} co-doped $CaMoO_4$ has been emitted green emission and not changed emitting color as Yb^{3+} concentrations, while UC phosphors such as Y_2O_3 [31] has been changed from green emission to red emission as Yb^{3+} doping concentrations.

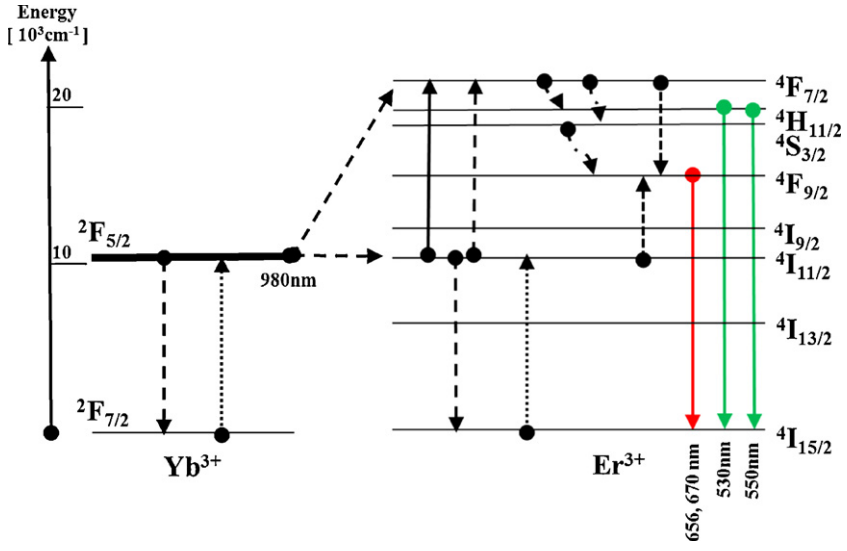

Fig. 6. Energy level diagrams of Er^{3+} and Yb^{3+} in $CaMoO_4$ and possible UC mechanisms under 980 nm excitation.

4. Conclusion

We synthesized Er^{3+}/Yb^{3+} co-doped $CaMoO_4$ UC phosphors by a complex citrate gel method. Under NIR excitation (980 nm), Er^{3+}/Yb^{3+} co-doped $CaMoO_4$ phosphors has obvious bright green UC luminescence at 530 and 550 nm with weak red emission at 656 and 670 nm. It was found that the UC emission intensity depends on Yb^{3+} acting as a sensitizer ion to improve the absorption cross-section around 980 nm, while Er^{3+} acts as an activator ion for UC luminescent centers in the $CaMoO_4$ matrix. The optimum doping concentrations of Er^{3+} and Yb^{3+} for highest green UC luminescence were 2 and 16 mol%, respectively. The UC emission is dominated by strong green emissions at 530 and 550 nm compared to red emissions at 656 and 670 nm which are resulted from the weak absorption cross-section of the $^4I_{13/2}$ level in Er^{3+} and the probability that electrons in the $^4I_{11/2}$ level get populated to the $^4F_{7/2}$ level via the ETU process, which is much higher than that of non-radiative relaxation to the $^4I_{13/2}$ level. Moreover, a two photon process is responsible for both the UC green luminescence generated by $^2H_{11/2}$, $^4S_{3/2} \rightarrow {}^4I_{15/2}$ and the red emission generated by $^2F_{7/2} \rightarrow {}^4I_{15/2}$ in Er^{3+}/Yb^{3+} co-doped $CaMoO_4$ phosphors. Therefore, based on our results, it was concluded that Er^{3+}/Yb^{3+} co-doped $CaMoO_4$ powders can be an excellent candidate for green UC phosphors.

Appendix A. Supplementary data

Supplementary data associated with this article can be found, in the online version, at doi:10.1016/j.jallcom.2012.01.059.

References

[1] J. Mendez-Ramos, V.K. Tikhomirov, V.D. Rodriguez, D. Furniss, J. Alloys Compd. 440 (2007) 328.
[2] J.H. Zhang, H.Z. Tao, Y. Chang, X.J. Zhao, J. Rare Earth 25 (2007) 108.
[3] T. Trupke, M.A. Green, P. Würfel, J. Appl. Phys. 92 (2002) 4117.
[4] B.S. Richards, A. Shalav, IEEE Trans. Electron Devices 54 (2007) 2679.
[5] E. Downing, L. Hesselink, J. Ralston, R. Macfarlane, Science 273 (1996) 1185.
[6] A. Rapaport, J. Milliez, M. Bass, A. Cassanho, H. Jenssen, J. Disp. Technol. 2 (2006) 68.
[7] X. Li, J.Y. Wang, J. Li, J. Lumin. 12 (2007) 351.
[8] H.X. Yang, H. Lin, Y.Y. Zhang, B. Zhai, E.Y.B. Pun, J. Alloys Compd. 453 (2008) 493.
[9] M. Liu, S.W. Wang, J. Zhang, L.Q. An, L.D. Chen, Opt. Mater. 29 (2007) 1352.
[10] J.C. Boyer, F. Vetrone, L.A. Cuccia, J.A. Capobianco, J. Am. Chem. Soc. 128 (2006) 7444.
[11] J.J. Owen, A.K. Cheetham, R.A. McFarlane, J. Opt. Soc. Am. B 15 (1998) 684.
[12] A.S. Oliveria, M.T. de Araujo, A.S. Gouveia, Appl. Phys. Lett. 72 (1998) 753.
[13] S.K. Singh, K. Kumar, S.B. Rai, Sens. Actuators A: Phys. 149 (2009) 16.
[14] R. Grasser, E. Pitt, A. Scharmann, G. Zimmerer, Phys. Status Solidi B 69 (1975) 359.
[15] D.A. Spassky, S.N. Ivanov, V.N. Kolobanov, V.V. Mikhailin, V.N. Zemskov, B.I. Zadneprovski, L.I. Potkin, Radiat. Meas. 38 (2004) 607.
[16] A. Phuruangrat, T. Thongtem, S. Thongtem, J. Alloys Compd. 481 (2009) 568.
[17] T. Thongtem, A. Phuruangrat, S. Thongtem, J. Ceram. Process. Res. 9 (2008) 189.
[18] L.H.C. Andrade, M.S. Li, Y. Guyot, A. Brenier, G. Boulon, J. Phys.: Condens. Matter 18 (2006) 7883.
[19] W. Sleight, Acta Crystallogr. B 28 (1972) 2899.
[20] J. Liu, H. Lian, C. Shi, Opt. Mater. 29 (2007) 1591.
[21] X-X. Luo, W.-H. Cao, J. Mater. Res. 23 (2008) 2078.
[22] D. Yang, C. Li, G. Li, M. Shang, X. Kang, J. Lin, J. Mater. Chem. 21 (2011) 5923.
[23] H. Guo, N. Dong, M. Yin, W. Zhang, L. Lou, S. Xia, J. Phys. Chem. B 108 (2004) 19205.
[24] Y. Bai, K. Yang, Y. Wang, X. Zhang, Y. Song, Opt. Commun. 281 (2008) 2930.
[25] F. Auzel, Chem. Rev. 104 (2004) 139.
[26] F. Wang, X. Liu, Chem. Soc. Rev. 38 (2009) 976.
[27] G.Y. Chen, H.C. Liu, H.J. Liang, G. Somesfalean, Z.G. Zhang, Solid State Commun. 196 (2008) 148.
[28] V. Singh, V.K. Rai, K.A. Shamery, J. Nordmann, M. Haase, J. Lumin. 131 (2011) 2679.
[29] Q. Sun, X. Chen, Z. Liu, F. Wang, Z. Jiang, C. Wang, J. Alloys Compd. 509 (2011) 5336.
[30] S. Das, A.A. Reddy, G.V. Prakash, Chem. Phys. Lett. 504 (2011) 206.
[31] H. Song, B. Sun, T. Wang, S. Lu, L. Yang, B. Chen, X. Wang, X. Kong, Solid State Commun. 132 (2004) 409.